Science and Technology Indonesia
e-ISSN:2580-4391 *p*-ISSN:2580-4405
Vol. 9, No. 1, January 2024

Research Paper

Optimization Thickness of Photoanode Layer and Membrane as Electrolyte Trapping Medium for Improvement Dye-Sensitized Solar Cell Performance

Nita Kusumawati[1*], Pirim Setiarso[1], Supari Muslim[2], Qonita Arky Hafidha[1], Sinta Anjas Cahyani[1], Fadlurachman Faizal Fachrirakarsie[1]

[1]*Department of Chemistry, Faculty of Mathematics and Natural Science, Universitas Negeri Surabaya, Surabaya, 60231, Indonesia*
[2]*Department of Electrical Engineering, Faculty of Engineering, Universitas Negeri Surabaya, Surabaya, 60231, Indonesia*
***Corresponding author**: nitakusumawati@unesa.ac.id

Abstract
Dye-Sensitized Solar Cells (DSSC) are photovoltaic devices that contain a dye that acts as a solar light acceptor. The use of dye-sensitized solar cells to solve increasing energy demand and environmental problems still results in low efficiency values. In this study, optimization of DSSC components was carried out to increase DSSC efficiency by varying the thickness of the titanium dioxide (TiO_2) semiconductor photoanode layer, polyvinylidene fluoride (PVDF) trap electrolyte membrane, and polyvinylidene fluoride nanofiber (PVDF NF) to obtain the optimum thickness. Scanning Electron Microscope (SEM) results of membrane thickness variation and titanium dioxide (TiO_2) semiconductor photoanode coating showed the formation of nanofiber fibers composed of three-dimensional, porous, and diameter networks connected to the PVDF NF membrane. The increase in density and decrease in pore size, along with an increase in thickness and cracking as the TiO_2 photoanode semiconductor layer increases, affect the electron transport rate of the DSSC. The higher particle density level will inhibit the electron transport rate, so it can reduce the efficiency of DSSC. The optimum thickness of the TiO_2 semiconductor layer and PVDF NF electrolyte membrane of 0.20 mm and 0.35 mm can produce values, voltage, fill factor current density, and electrical efficiency of 500 mV, 2.7 x 10^{-3} mA.cm^{-2}, 1.80%, and 2.40%, respectively.

Keywords
DSSC, Electrolyte, PVDF, PVDF NF, Photoanode, Titanium Oxide

Received: 18 May 2023, Accepted: 14 September 2023
https://doi.org/10.26554/sti.2024.9.1.7-16

1. INTRODUCTION

Energy is the main need for human life (Diantoro et al., 2020). The need related to energy demand is expected to increase while the availability of energy, especially fossil fuels, is insufficient, so solar energy is needed as an environmentally friendly alternative energy source (Esgin et al., 2022; Khan et al., 2022). Moreover, the sun can deliver up to 120.000 kW before it reaches the surface of the earth, which is 6.000 times the world's energy consumption today (Esgin et al., 2022; Dambhare et al., 2021). One type of solar cell that has attracted the interest of researchers is the dye-sensitized solar cell (DSSC) because the fabrication process is relatively easy with low cost and can convert power with relatively high efficiency (Tontapha et al., 2021).

The DSSC consists of a photosensitizer, electrolyte, transparent conducting oxide film (TCOs), the counter electrode, and a semiconductor metal-oxide film electrode (Karim et al., 2019; Semalti and Sharma, 2020). The DSSC mechanism is based on the absorption of the dye by the semiconductor as a free reservoir of electrons when sunlight comes, and the electrons disparate to the edge of the semiconductor's band gap before entering the conduction band, which limits the main recombination process, causing lower charge rates and higher solar cell efficiency (Abdel-Galeil et al., 2021).

The effectiveness of DSSC performance is influenced by various factors, such as the composition of the counter-electrode material, the type of dye used, the type of electrolyte, and the morphology and structure of the photoanode (Richhariya et al., 2022). Several studies regarding the use of TiO_2 have investigated the impact of varying the thickness of TiO_2 on cell efficiency. These investigations revealed that thicker layers increased pigment absorption, increased photon injection, and increased electron excitation (Shirkavand et al., 2019). However, this widens the gap between TiO_2 and FTO, causing delayed electron passage, more recombination time, and a reduced electron injection rate to generate electricity (Abdel-Galeil et al., 2021). Therefore, it is important to study the thickness of the TiO_2 layer which can increase the efficiency of DSSC.

The electrolyte also has a notable role in determining stability in DSSC systems (Semalti and Sharma, 2020). In general, the electrolyte commonly used is a liquid electrolyte with higher efficiency compared to solid and gel electrolytes, but it has a leakage, high volatility, corrosion of the opposing electrode, airtight cell sealing, and iodine sublimation often occur so that the stability of this solar cell has a short term (Dissanayake et al., 2021; Drygała, 2021; Ammar et al., 2019). To overcome the stability problem of DSSC, polymer electrolyte was developed with a solid and network structure that can provide good thermal stability and ionic conductivity approaching that of liquid electrolytes (Semalti and Sharma, 2020; Drygała, 2021).

In polymer electrolytes, poly-vinylidene fluoride (PVDF) is favored by strong electron-withdrawing functional groups (-C-F), high dielectric constant values, excellent mechanical strength, stability to corrosive materials, low ionic radius, and electronegativity. Each is very high, resulting in good ion transport and low recombination rates between the photo-anode and the electrolyte (Liu et al., 2021; Saxena and Shukla, 2021). However, the ionic mobility of the I^-/I_3 ions is reduced by their hydrophobic nature. Thus, PVDF NF membranes are made as an alternative to increasing ionic mobility in PVDF observation. With an amorphous structure that dominates the PVDF NF membrane, it can produce a higher ionic conductivity value than the PVDF membrane (Kusumawati et al., 2023).

In this study, we evaluated the TiO_2 paste thickness and the polymer electrolyte thickness based on the PVDF NF membrane using the *telang* flower as the best natural photo-sensitizer to increase efficiency and stability in the DSSC system. Both parameters are characterized by observing the surface and cross-sectional morphology of TiO_2 photo-anode film, PVDF, and PVDF NF membranes utilizing Scanning Electron Microscopy (SEM) on the Zeiss EVO MA-10. The efficiency of the DSSC was analyzed based on the voltage and current received from measurements using a Krisbow KW08-267 Multimeter (200 mV and a resistance of 200 kΩ).

2. EXPERIMENTAL SECTION

2.1 Materials

The materials and their specifications used in this study were KI (potassium iodide) (Merck, Belgium; ≥99%); EC (ethylene carbonate) (Sigma Aldrich, USA; anhydrous 99%); PC (propylene carbonate) (Sigma Aldrich, USA; anhydrous 99.7%); Iodine (Sigma Aldrich, Singapore; ≥99.8%); Poly(vinylidene fluoride) (PVDF) (Sigma Aldrich, Singapore; powder, Mw 534,000); acetone (Sigma Aldrich, Germany; ≥99.5%); DMAc (N,N-Dimethylacetamide) (Merck, Belgium; ≥99%); TiO_2 (Sigma Aldrich, China; 21 nm nanopowder; 99.5%); PEG (polyethylene glycol) (Sigma Aldrich, Germany Mw 1000); Tween-80 (PT. Brataco Chemika; Indonesia); and FTO glass (resistivity 10); HNO_3(Sigma Aldrich, Germany; ≥99.9%).

The surface and cross-section morphology of the PVDF, PVDF NF, and TiO_2 films were analyzed using a Zeiss EVO MA-10 SEM. The DSSC circuit's efficiency was evaluated using current and voltage measurements collected with a Krisbow KW08-267 Multimeter at 200 mV voltage and 200 kΩ resistance.

2.2 Methods

2.2.1 Making of Pasta TiO_2

TiO_2 pasta was made by combining 0.2 g titanium oxide (TiO_2), 0.08 g propylene glycol (PEG-1000), 0.4 mL 0.1 M nitric acid (HNO_3) solution, and 0.05 mL of tween-80, stirred for 30 minutes at 100 rpm (Kusumawati et al., 2023).

2.2.2 Natural Dye Sensitizer

Making a natural dye sensitizer using the maceration method. The natural sensitizer dye used is dried *telang* flowers. In a 1:6 ratio, dried *telang* flowers were immersed in distilled water. Evaporate the filtrate of maceration using a Buchi R-300 rotary evaporator. The evaporated concentrate was kept at 20-25 °C room temperature (Kusumawati et al., 2023).

2.2.3 Polymer-electrolyte Membrane

Making a polymer-electrolyte membrane is carried out in two steps, first making an electrolyte solution and then making a PVDF membrane. The electrolyte solution was made by mixing 9.2 mg solid iodine (I_2), 0.06 g potassium iodide, 0.4 g propylene carbonate (PC), and 0.4 g ethylene carbonate (EC) using a magnetic stirrer NESCO LAB MS-H280-Pro magnet at 100 rpm for 30 minutes. PVDF membranes are created using a phase separation procedure, electrospinning and casting knife methods. PVDF was dissolved in a 3:2 combination of DMAc and acetone using a hot plate magnetic stirrer at 65 °C temperature and 270 rpm speed for 12 hours to produce an 18% (w/v) PVDF solution. Membrane with casting knife technique: 18% (w/v) PVDF solution was cast on glass with a thickness variation of 0.6 mm, 0.4 mm, and 0.2 mm at a 30 °C temperature with an initial immersion time of 5 minutes, then immersed in 1000 mL of water distillate non-solvent coagulation bath at a 30 °C temperature for 30 minutes. Next, the solid PVDF membrane was washed in 500 mL of non-solvent distilled water for 1 minute 2 times and allowed to rest for 24 hours at 25 °C room temperature. Membrane with electrospinning casting technique: 18% (w/v) PVDF solution was processed with variations in 5 cm, 10 cm, and 15 cm distances between the injection and the drum collector, a flow rate of 1 mL/hour, and a voltage of 15 kV for 5 hours.

2.2.4 Fabrication DSSC

The DSSC is made up of two FTO glasses (anode + cathode). The active surface area of the FTO anode glass is 3 cm^2. A doctor blade was used to cover TiO_2 paste on glass, which was sintered for 1 hour at 450 °C temperature. The TiO_2 photo-anode was allowed to cool and then submerged for 24 hours in 10 mL of natural dye. The membranes were deposited on a carbon-coated cathode FTO glass after being submerged in 1 mL of electrolyte for 1 hour. As a result, the system of FTO/TiO_2/PVDF/Pt/FTO is created.

3. Results and Discussion

3.1 Solid Electrolyte

The electrolyte is a significant component in the DSSC as an internal charge carrier between the metal oxide and the electrode (Yang et al., 2022). In the application of the DSSC circuit, there are 3 types of electrolytes, namely liquid, solid, and quasi-solid states. Liquid electrolytes have high ionic conductivity values but are easily leaky and volatile (Lobregas and Camacho, 2019). Solid polymer electrolyte, compared to other electrolytes, provides good heat resistance, and ionic conductivity and increases the long-term stability of DSSC (Liu et al., 2020; Semalti and Sharma, 2020).

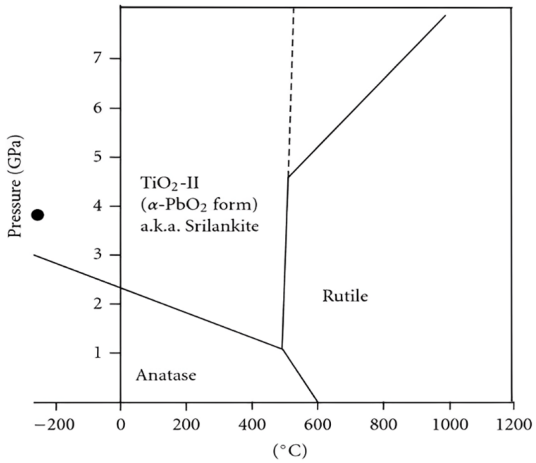

Figure 1. Crystal Structure of Titanium Dioxide (TiO_2)

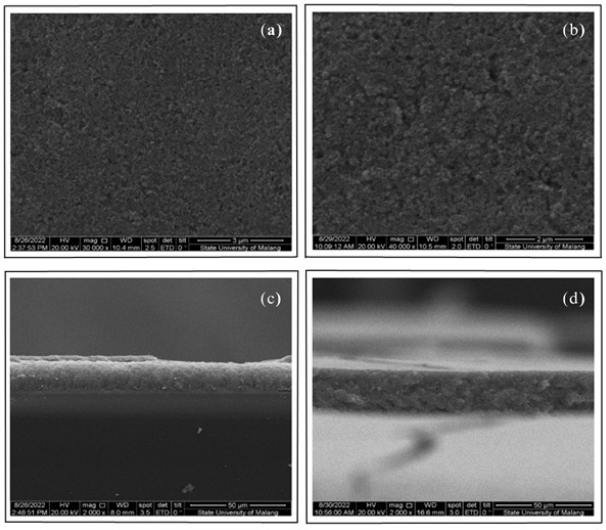

Figure 2. TiO_2 Film Surface Morphology ((a) 0.2 mm, (b) 0.6 mm)) and Cross-Section ((c) 0.2 mm and (d) 0.6 mm))

In the manufacture of polymer electrolytes, it is carried out before the manufacture of membranes made of PVDF which

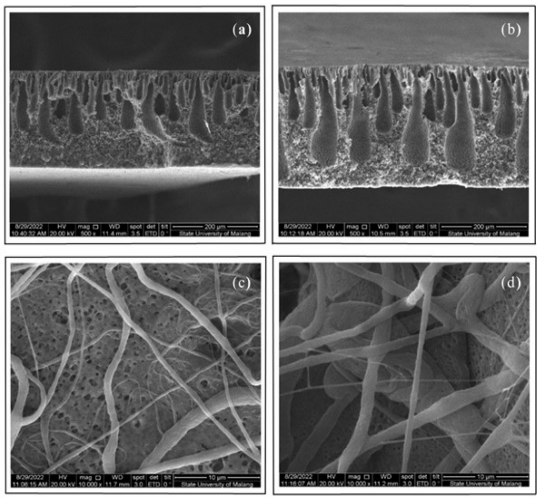

Figure 3. Polymer Electrolyte: Cross-section 500x; (a) PVDF 0.2 mm, (b) PVDF 0.6 mm and Surface Morphology 30.000x; (c) PVDF NF 0.35 mm, (d) PVDF NF 0.45 mm

is a membrane with superior thermal resistance and asymmetrical structure with low mass transfer resistance to minimize fouling (Kusumawati et al., 2018). The manufacturing process is simple and flexible, using the phase inversion method with non-water solvents and then casted in thicknesses (0.2 mm, 0.4 mm, and 0.6 mm). It is reported that the high differences in the solubility values of PVDF-water (15.88 MPa½), DMAc-water (25.23 MPa½), and acetone-water (28.30 MPa½) disrupted the thermodynamic balance of the PVDF-DMAc and PVDF-acetone systems, triggering phase separation to form PVDF membranes solid (Kusumawati et al., 2023).

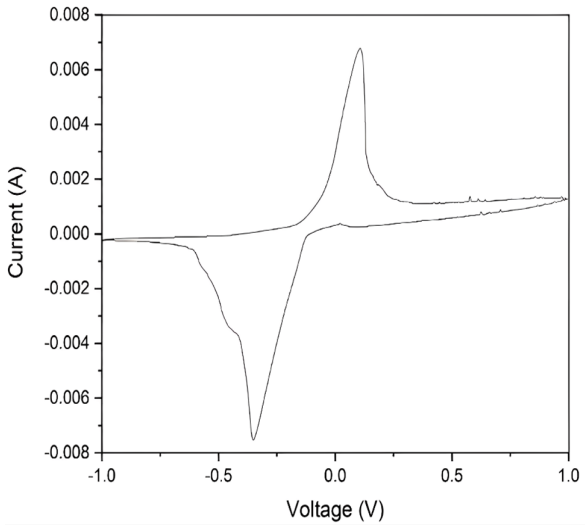

Figure 4. Voltammogram of *Telang* Flower Extract as a DSSC Photosensitizer

In addition, the manufacture of PVDF nanofiber mem-

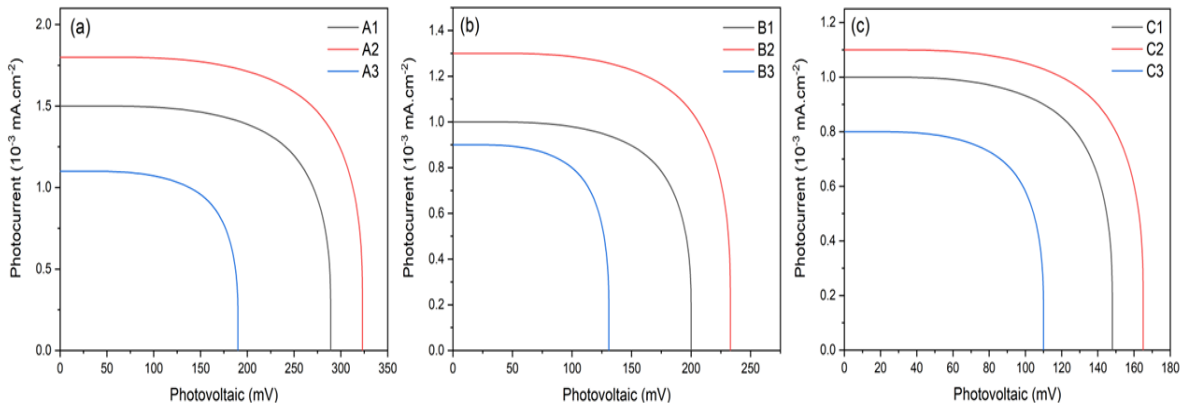

Figure 5. I-V Curve of Variation of the Thickness of the PVDF Membrane on the TiO_2 Layer with a Thickness of; (a) 0.2 mm, (b) 0.4 mm, (c) 0.6 mm

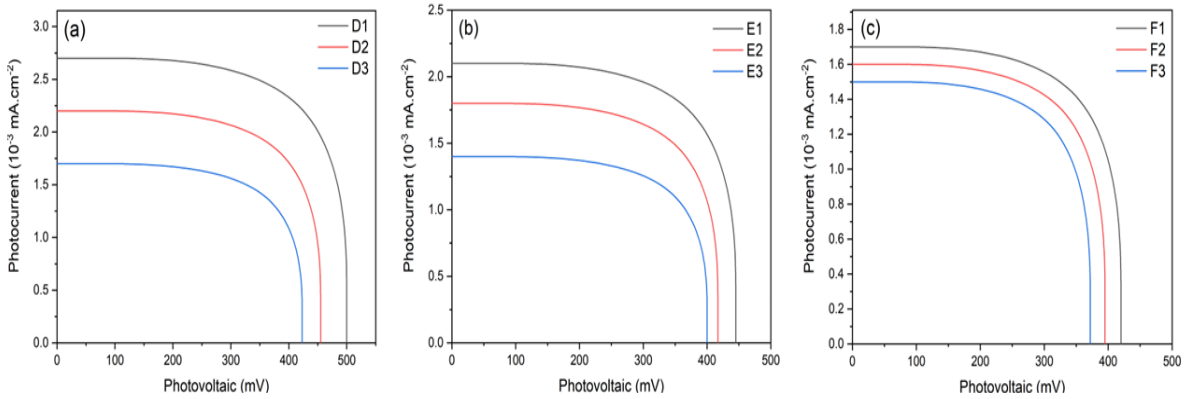

Figure 6. I-V Curve of Variation of the Thickness of the PVDF NF Membrane on the TiO_2 Layer with a Thickness of; (a) 0.35 mm, (b) 0.40 mm, (c) 0.45 mm

branes with a hollow structure was made using the electrospinning method. PVDF was dissolved in DMAc and acetone in a ratio of 3:2, stirred for 12 hours at 65 °C then varied in thickness by varying the spinneret-collector distance; 5 cm, 10 cm, and 15 cm (Kusumawati et al., 2023). At a constant stress, the spinning distance between the spinneret–collectors affects the fiber strain and deposition which causes differences in the thickness of the PVDF Nanofiber (PVDF NF) produced. The short spinning distance causes fiber stretching and insufficient dissolution so that the resulting thick membrane has coarse and porous fibers (Zhang et al., 2021). While the long spinning distance causes thin membranes because the polymer solution will evaporate faster before reaching the drum collector. By varying the spinneret-gatherer spinning distance, the 5 cm, 10 cm, and 15 cm thickness of the NF PVDF membrane respectively were 0.35 mm, 0.40 mm, and 0.45 mm.

3.2 Photo-anode Layer

The photo-anode layer is one of the significant components of the DSSC (Padmini et al., 2021). This layer has a role in the absorption of dyes in the DSSC. The dye that is absorbed and attached to the surface of the photo-anode layer will absorb photos from sunlight, and then electrons will be excited by the conduction band (Zhou et al., 2022). Thus, to optimize the performance of the photo-anode layer in the DSSC system, a semiconductor material that has a wide surface area is needed to increase the absorption capacity of the dye, interface contact between dye molecules and the conductive layer, fast electron transfer, suitable pore size to facilitate dye diffusion, high resistance to photo-corrosion, ability to absorb or diffuse sunlight, and good electron-accepting ability (Padmini et al., 2021).

In general, semiconductor materials for DSSC cells include titanium dioxide (TiO_2), magnesium oxide (MgO), zinc oxide (ZnO), and tin (IV) oxide (SnO_2). Zinc oxide (ZnO) material has better electron mobility than titanium dioxide, but the resulting efficiency is lower than titanium dioxide. This is due to

Table 1. Voltammetric Parameters of *Telang* Flower Anthocyanin Pigment

Dye	E_{ox} (eV)	HOMO (eV)	Ered (eV)	LUMO (eV)	Band gap (eV)
Telang flower	0.1037	-4.2963	-0.3489	-4.0511	0.2452

the low ability of ZnO to absorb dyes and the lack of stability in an acidic environment, so the selected semiconductor material is titanium oxide (Hossain et al., 2019). The choice of titanium oxide (TiO_2) as a semiconductor material depends on its physicochemical properties such as surface area, crystal structure, grain size, grain boundary density, energy band gap, cost efficiency, good stability, affordability, optical/electronic properties, compatibility, and non-toxicity (Drygała, 2021; Padmini et al., 2021). The type of semiconductor contained in titanium dioxide is anatase, which has high catalytic activity against sunlight (Medvids et al., 2021; Xie et al., 2022). With a high surface area and nanocrystal structure, titanium dioxide can increase its density and electron transfer.

The titanium dioxide photo-anode layer was made using the doctor blade method because of its flexibility and cost-effectiveness (Padmini et al., 2021). The TiO_2 semiconductor layer was made in three thickness variations, namely 0.6 mm, 0.4 mm, and 0.2 mm, and then calcined at a temperature of 450 °C for 1 hour.

Based on Figure 1, titanium dioxide (TiO_2) has three crystal structures: anatase, rutile, and brookite, with the main phases being anatase and rutile (Zhang et al., 2021; Sabzi and Anijdan, 2019). At high temperatures, the anatase phase can change to the rutile phase. The transition from the anatase phase to the rutile phase occurs at temperatures between 600 °C and 1000 °C (Boytsova et al., 2022). Since the surface area of anatase is larger than that of rutile, most DSSCs still use the anatase crystal structure, but rutile TiO_2 has several advantages over anatase, such as higher chemical stability and a higher refractive index (Vural, 2020).

3.3 Scanning Electron Microscopy (SEM)

The surface morphology of the TiO_2 paste and film layers (both PVDF and PVDF-NF membranes) was observed using scanning electron microscopy (SEM) (Benhabiles et al., 2019). Surface detection of the TiO_2 layer is very important for dye adsorption on DSSCs. Due to the large surface area, optimal pore diameter and pore volume can improve DSSC performance (Venkatesan et al., 2022). Figure 2 shows the results of the SEM test on the resulting TiO_2 paste layers with thickness variations of 0.2 mm and 0.6 mm.

Based on Figure 2, the results of the SEM test at all thicknesses showed a uniformly smooth, and free of cracks on the surface (Drygała, 2021). In the research of Drygała (2021) on the effect of thickness variations on photovoltaic values, DSSC also reported that the surface morphology of all TiO_2 paste layer thicknesses was uniform in the distribution of the material. The surface morphology and the thickness of the titanium oxide semiconductor layer show no significant difference, but it is clear that there are cracks at a thickness of 0.6 mm. While the cross-sectional SEM image of the titanium oxide layer, which is 0.2 mm thick, has a nanoporous structure that is thinner than the nanoporous structure at 0.6 mm thickness of the titanium oxide layer.

Titanium dioxide (TiO_2) nanoparticles calcined at 400 °C have a spherical shape with small nanoparticle sizes in the range of less than 18 nm (Lal et al., 2021). The output showed that the resulting pore size was very small. However, there is a defect in the presence of holes in the thickness of the TiO_2 nanoparticles. This will make it easier for the solution to cause damage, causing a larger hole. In the 0.2 mm TiO_2 layer, the resulting defects are smaller than the 0.6 mm TiO_2.

The exponent increases suddenly when increasing the thickness of the DOS (Density of State) defect formation, which is increased by the increase in the amorphous phase, fraction. Thus, of course, the volume of TiO_2 is dependent on dependence. The thinner the TiO_2, the lower the fraction of the amorphous phase which is an irregular solid. When dense with current density, impedance occurs in the state of a small amorphous fraction. This shows that to reduce the amorphous phase, the thickness of TiO_2 must be reduced to a certain value.

Based on Figure 3, the surface of the PVDF membrane shows a porous structure. The porous structure looks smaller as the membrane thickness increases. Meanwhile, the surface of the PVDF NF membrane shows different porous fibers for each thickness. Membranes consisting of thinner nanofibers have a clear pore size (Lobregas and Camacho, 2019). SEM cross-section images of PVDF membranes with dissimilar thickness, are 0.2 mm and 0.6 mm. Based on the Figure 3, the thicker the PVDF membrane, the greater the particle density. The particle density of the electrolyte-trapping polymer affects the flow rate of electrons in charge transport. The greater the level of particle density, the driving force for passing particles through the membrane is large and the speed of the feed solution in passing through the membrane is lower so that the flow rate of electrons in the charge transport that occurs will be slower, resulting in an efficiency reduction of the DSSC (Semalti and Sharma, 2020). Thus, the PVDF membrane thickness as an electrolyte trap affects the flow rate of electrons in charge transport which has an influence on the efficiency of the DSSC.

To achieve high efficiency of solar cells with high mechanical stability of the film, the existence of crosslinks inside the nanofiber network is one of the key parameters. The density of the polymer particles that capture electrolytes affects the slow flow rate of electrons in the charge transport that oc-

Table 2. Photovoltaic Analysis of DSSC with Variations in PVDF Membrane Thickness

Code	TiO_2 Thickness (mm)	PVDF Membrane Thickness (mm)	J_{sc} ($mA.cm^{-2}$)	V_{oc} (mV)	FF (%)	η (%)
A1		0.20	1.5×10^{-3}	289	0.80	1.15
A2	0.20	0.40	1.8×10^{-3}	323	0.95	1.57
A3		0.60	1.1×10^{-3}	190	0.70	0.86
B1		0.20	1.0×10^{-3}	200	0.65	0.86
B2	0.40	0.40	1.3×10^{-3}	233	0.70	1.10
B3		0.60	0.9×10^{-3}	131	0.63	0.70
C1		0.20	1.0×10^{-3}	148	0.52	0.71
C2	0.60	0.40	1.1×10^{-3}	165	0.61	0.74
C3		0.60	0.8×10^{-3}	110	0.45	0.50

Table 3. Photovoltaic Analysis of DSSC with Variations in PVDF Nanofiber (NF) Membrane Thickness

Code	TiO_2 Thickness (mm)	PVDF Membrane Thickness (mm)	J_{sc} ($mA.cm^{-2}$)	V_{oc} (mV)	FF (%)	η (%)
D1		0.35	2.7×10^{-3}	500	1.80	2.40
D2	0.20	0.40	2.2×10^{-3}	455	1.88	1.85
D3		0.45	1.7×10^{-3}	423	1.87	1.32
E1		0.35	2.1×10^{-3}	445	1.93	1.81
E2	0.40	0.40	1.8×10^{-3}	417	1.97	1.48
E3		0.45	1.4×10^{-3}	400	1.88	1.05
F1		0.35	1.7×10^{-3}	420	1.68	1.22
F2	0.60	0.40	1.6×10^{-3}	395	1.71	1.08
F3		0.45	1.5×10^{-3}	372	1.61	0.90

curs so it has an impact on decreasing the performance of the DSSC. Furthermore, the greater the level of particle density, the lower the driving force needed to pass the particles through the membrane. Therefore, the electrolyte-trapping polymer in the PVDF NF has a potential application in DSSC compared to PVDF (Kusumawati et al., 2023).

3.4 Photovoltaic Studies

In the DSSC system, several components as a result the current and voltage values of the DSSC make up the DSSC system including transparent conducting oxide film (TCO) in the form of FTO glass, semiconductor metal oxide electro-film as a photo-anode (TiO_2 nanoparticles), dye as a photo-sensitizer, I/I_3- based electrolyte as a mediator electrode, and counter electrodes such as carbon, is commonly used because they are cheap. The principle of DSSC is based on the dye as a light absorber (photo-sensitizer) and a semiconductor layer as a charge separation site (Diantoro et al., 2020).

To become a DSSC photosensitizer, the dye must have a narrower bandgap energy than the semiconductor energy (TiO_2; 3.2 eV for anatase and 3.0 eV for the rutile phase) so as to produce high efficiency. The bandgap energy can be determined from the HOMO (Highest Occupied Molecular Orbital) and LUMO (Lowest Occupied Molecular Orbital) energy values, which are characterized using the cyclic voltammetry method. The determination of the dye band gap energy follows the equation (Kusumawati et al., 2023; Setiarso et al., 2023):

$$E_{HOMO} = -e\ (Eox + 4.4)\ eV \quad (1)$$

$$E_{LUMO} = -e\ (Ered + 4.4)\ eV \quad (2)$$

$$Eg = E_{LUMO} - E_{HOMO}$$

In this study, electrochemical characterization of anthocyanin pigments from *telang* flower was carried out under acid conditions at pH 1, resulting in the following voltammogram:

In Figure 4, the E_{ox} is obtained from the I_{pa} peak and the E_{red} from the I_{pc} peak, so that the HOMO and LUMO values are obtained in Table 1.

Dyes possessing a narrow band gap energy exhibit electrons with greater excitation potential, leading to an enhancement in

Table 4. Photovoltaic Analysis of DSSC with Variations Titanium Oxide (TiO_2) Photo-anode Film Thickness in PVDF Membrane

Code	TiO_2 Thickness (mm)	PVDF Membrane Thickness (mm)	J_{sc} ($mA.cm^{-2}$)	V_{oc} (mV)	FF (%)	η (%)
G1		0.20	1.5×10^{-3}	292	1.10	1.40
G2	0.20	0.40	1.0×10^{-3}	205	1.12	0.86
G3		0.60	0.9×10^{-3}	148	0.91	0.70
H1		0.20	1.7×10^{-3}	320	0.92	1.45
H2	0.40	0.40	1.3×10^{-3}	234	0.90	1.03
H3		0.60	1.1×10^{-3}	165	0.81	0.75
I1		0.20	1.1×10^{-3}	288	0.82	0.83
I2	0.60	0.40	0.9×10^{-3}	132	0.72	0.67
I3		0.60	0.8×10^{-3}	111	0.69	0.50

Table 5. Photovoltaic Analysis of DSSC with Variations Titanium Oxide (TiO_2) Photo-anode Film Thickness in PVDF Nanofiber (NF) Membrane

Code	TiO_2 Thickness (mm)	PVDF Membrane Thickness (mm)	J_{sc} ($mA.cm^{-2}$)	V_{oc} (mV)	FF (%)	η (%)
J1		0.20	2.5×10^{-3}	498	1.77	2.21
J2	0.35	0.40	2.1×10^{-3}	447	1.87	1.79
J3		0.60	1.8×10^{-3}	421	1.71	1.32
K1		0.20	2.0×10^{-3}	450	1.93	1.74
K2	0.40	0.40	1.7×10^{-3}	420	1.89	1.35
K3		0.60	1.5×10^{-3}	387	1.71	1.03
L1		0.20	1.8×10^{-3}	420	1.86	1.38
L2	0.45	0.40	1.4×10^{-3}	405	1.84	1.07
L3		0.60	1.3×10^{-3}	365	1.68	0.82

their sensitivity to light. Anthocyanin pigments are dyes with many conjugated bonds. The greater the number of conjugated chains, the more prolonged the electron resonance between the donor and acceptor structures, consequently resulting in a narrower band gap energy. As a result, the anthocyanin pigment derived from *telang* flower extract holds significant promise as a dye for enhancing the performance of DSSCs (Kusumawati et al., 2023). Table 1 shows the narrow band gap energy value of *telang* flower extract at pH 1, which amounted to 0.2452 eV. While in research Kusumawati et al. (2023), *telang* flower extract in neutral conditions produces a band gap of 1.182 eV. This indicates that *telang* flower anthocyanin pigments in acidic conditions have a higher potential to improve DSSC performance than in neutral conditions.

The semiconductor layer of the TiO_2 paste and electrolyte is a determinant of the assessment of the performance of the DSSC system. The electrolyte membrane thickness and the optimum thickness of TiO_2 paste for the DSSC are determined from the results of the analysis of voltage at open circuit (V_{oc}), charge factor (FF), efficiency (η), and short circuit current density (J_{sc}) based on the following equation:

$$\eta = \frac{J_{sc} V_{oc} FF}{P_{in}} \times 100\% \tag{3}$$

$$FF = \frac{P_{max}}{J_{sc} V_{oc}} = \frac{I_{max} V_{max}}{J_{sc} V_{oc}} \tag{4}$$

Based on Table 2 and shown in the I-V curve of Figure 5, the thickness of the polymer membrane as a trapping medium for electrolyte solutions affects the photovoltaic parameter values for DSSC cell circuits. The optimal thickness of the PVDF membrane is 0.4 mm. This is influenced by the density and pore size of the membrane, thicker polymer membrane, smaller pore size, and higher particle density so that the electrolyte solution trapped in the membrane will reduce the flow rate of electrons in the slower charge transport so that the current and voltage values in the circuit will be lower. DSSC is getting smaller. While the thickness of 0.2 mm has a low particle density, the pore size is large so that the flow rate will run faster and the electrolyte will more easily penetrate the

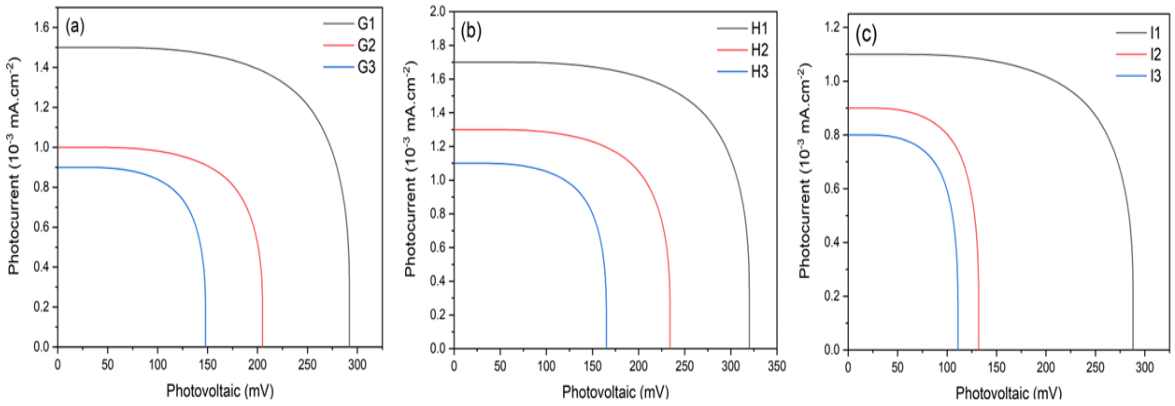

Figure 7. I-V Curve of TiO_2 Layer Thickness Variation on a PVDF Membrane with a Thickness of; (a) 0.2 mm, (b) 0.4 mm, (c) 0.6 mm

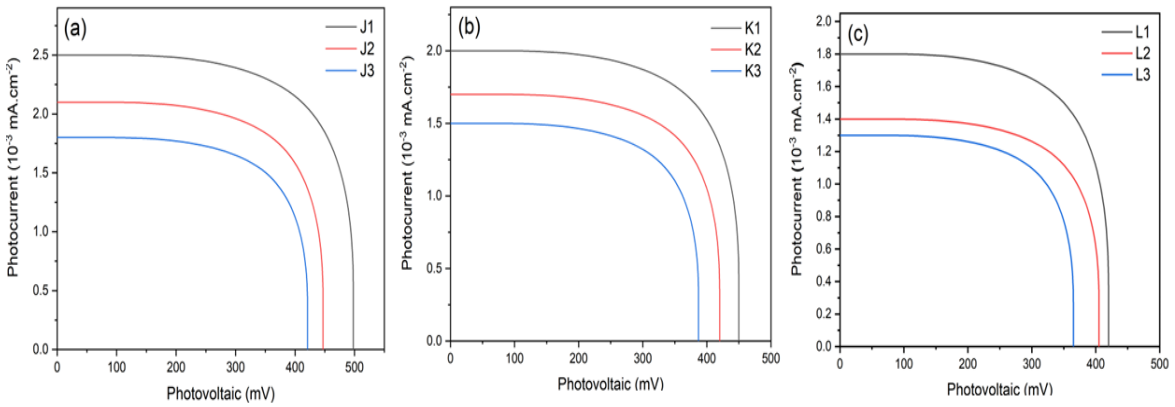

Figure 8. I-V Curve of TiO_2 Layer Thickness Variation on a PVDF NF Membrane with a Thickness of; (a) 0.35 mm, (b) 0.40 mm, (c) 0.45 mm

membrane so that it can cause less leakage, as a result, the current and voltage values of the DSSC system are less than optimal. To determine the optimal membrane thickness by cross-linking, which produces an optimal PVDF membrane thickness of 0.4 mm.

To increase the current and voltage values, a nanofiber PVDF membrane with a hollow structure was made using the electrospinning method. PVDF was dissolved in DMAc and acetone in a ratio of 3:2, stirred for 12 hours at 65 °C then varied in thickness by varying the spinneret-collector distance: 5 cm, 10 cm, and 15 cm (He et al., 2021). The effect of the distance between the spinneret-collector causes differences in the thickness of the resulting PVDF NF membrane. The farther the spinneret-collector distance, the thinner the PVDF NF membrane because the polymer solution will evaporate faster before reaching the collector drum, and vice versa, the closer the spinneret-collector distance, the thicker the PVDF NF membrane produced will be. Thus, the spinneret-collector distance of 5 cm, 10 cm, and 15 cm resulted in PVDF NF membrane thicknesses of 0.45 mm, 0.40 mm, and 0.35 mm.

Based on Table 3 photovoltaic analysis of DSSC cell circuits with variations in PVDF NF membrane thickness, the thickness of the polymer membrane as a trapping medium for the electrolyte solution affects the value of each photovoltaic parameter in the DSSC cell circuit. The thicker the PVDF NF membrane, the higher the membrane density. The high density of the membrane results in low elasticity properties, so the rate of electrons in charge transport moves slower. Thus, the electrical efficiency values of the DSSC decrease, and vice versa by the thinner membrane and the lower membrane density. The low density of the membrane causes electrons to move easily, so that the rate of electron charge transport is faster. As a result, the value of electrical efficiency obtained is large. Thus, the optimal PVDF NF membrane thickness for the DSSC system is 0.35 mm. Moreover, the impact of changing the thickness of the PVDF NF membrane on the performance of DSSCs using natural photosensitizers can be seen in the current-voltage curve depicted in Figure 6.

Based on Table 4 photovoltaic analysis of DSSC cells with variations in TiO_2 layer thickness on PVDF membranes and Table 5 photovoltaic analysis of DSSC cells with variations in TiO_2 layer thickness on PVDF NF membranes, the optimal thickness of the titanium oxide semiconductor layer was 0.2 mm. The thicker the titanium oxide semiconductor layer, the more cracked or shrinking the layer will be, so that the dye absorption is not optimal. This is caused by high-temperature heating. In addition, the large total surface area in the structures of nanoporous can lead to higher electron transport series resistance, causing the recombination of the electrons with I_{3^-} ions on the TiO_2 surface, resulting in low-efficiency values (Shirkavand et al., 2019). The effect of TiO_2 layer thickness variation on DSSC performance is confirmed by the current-voltage curves shown in Figure 7 and Figure 8.

4. CONCLUSION

The manufacture of PVDF membranes and TiO_2 layers with various thicknesses has been done. The results of SEM PVDF with variations in thickness show that the thickness of the PVDF membrane to trap the electrolyte affects the flow rate of electrons in charge transport, which has an impact on the efficiency of the DSSC circuit system. The higher the level of particle density, the greater the driving force for passing particles through the membrane is large and the speed of the feed solution in passes through the membrane, the slower the flow rate of electrons in the charge transport that occurs, which can reduce the value of electrical efficiency. While variations in the thickness of the PVDF NF membrane show that the thicker the PVDF NF membrane, the higher the membrane density. The high density of the membrane results in low elasticity properties, so the rate of electrons in charge transport moves slower. Thus, the value of the electrical efficiency of the DSSC decreases. The TiO_2 layer with thickness variations of 0.2 mm, 0.4 mm, and 0.6 mm, the surface layers are not much different. The large total surface area in the nanoporous structure can lead to higher electron transport series resistance, causing the recombination of electrons with I_{3-} ions on the TiO_2 surface, resulting in low-efficiency values. Thus, the optimal thickness of the PVDF membrane and titanium oxide layer to improve DSSC performance is 0.35 mm and 0.2 mm with an electrical efficiency value of 2.40%.

5. ACKNOWLEDGEMENT

The authors would like to thank the Ministry of Education, Culture, Research, and Technology of the Republic of Indonesia for financial support with the contract number of 948/UN38/HK/KP/2023.

REFERENCES

Abdel-Galeil, M. M., R. Kumar, A. Matsuda, and R. E. El-Shater (2021). Investigation on Influence of Thickness Variation Effect of TiO_2 Film, Spacer and Counter Electrode for Improved Dye-Sensitized Solar Cells Performance. *Optik*, **227**(166108); 166108

Ammar, A. M., H. S. Mohamed, M. M. Yousef, G. M. Abdel-Hafez, A. S. Hassanien, and A. S. Khalil (2019). Dye-Sensitized Solar Cells (DSSCs) Based on Extracted Natural Dyes. *Journal of Nanomaterials*, **2019**; 1–10

Benhabiles, O., F. Galiano, T. Marino, H. Mahmoudi, H. Lounici, and A. Figoli (2019). Preparation and Characterization of TiO_2-PVDF/PMMA Blend Membranes using an Alternative Non-Toxic Solvent for UF/MF and Photocatalytic Application. *Molecules*, **24**(4); 724

Boytsova, O., I. Zhukova, A. Tatarenko, T. Shatalova, A. Beiltiukov, A. Eliseev, and A. Sadovnikov (2022). The Anatase-to-Rutile Phase Transition in Highly Oriented Nanoparticles Array of Titania with Photocatalytic Response Changes. *Nanomaterials*, **12**(24); 4418

Dambhare, M. V., B. Butey, and S. Moharil (2021). Solar Photovoltaic Technology: A Review of Different Types of Solar Cells and Its Future Trends. In *Journal of Physics: Conference Series*, volume 1913. IOP Publishing, page 012053

Diantoro, M., M. B. Zaini, T. Suprayogi, N. Mufti, S. Zulaikah, and A. Hidayat (2020). Effect of (SnO_2: TiO_2) Nanoparticles on Charging Performance of Integrated Dye-Sensitized Solar Cell-Supercapacitor. In *AIP Conference Proceedings*, volume 2231. AIP Publishing

Dissanayake, M., T. Jaseetharan, G. Senadeera, B. Mellander, I. Albinsson, M. Furlani, and J. Kumari (2021). Solid-State Solar Cells Co-Sensitized with PbS/CdS Quantum Dots and N719 Dye and Based on Solid Polymer Electrolyte with Binary Cations and Nanofillers. *Journal of Photochemistry and Photobiology A: Chemistry*, **405**(112915); 112915

Drygała, A. (2021). Influence of TiO_2 Film Thickness on Photovoltaic Properties of Dye-Sensitized Solar Cells. In *IOP Conference Series: Earth and Environmental Science*, volume 642. IOP Publishing, page 012001

Esgin, H., Y. Caglar, and M. Caglar (2022). Photovoltaic Performance and Physical Characterization of Cu Doped ZnO Nanopowders as Photoanode for DSSC. *Journal of Alloys and Compounds*, **890**(161848); 161848

He, Z., F. Rault, M. Lewandowski, E. Mohsenzadeh, and F. Salaün (2021). Electrospun PVDF Nanofibers for Piezoelectric Applications: A Review of the Influence of Electrospinning Parameters on the β Phase and Crystallinity Enhancement. *Polymers*, **13**(2); 174

Hossain, M. K., M. Rahman, M. Basher, M. Manir, and M. Bashar (2019). Influence of Thickness Variation of Gamma-Irradiated DSSC Photoanodic TiO_2 Film on Structural, Morphological and Optical Properties. *Optik*, **178**; 449–460

Karim, N. A., U. Mehmood, H. F. Zahid, and T. Asif (2019). Nanostructured Photoanode and Counter Electrode Materials for Efficient Dye-Sensitized Solar Cells (DSSCs). *Solar Energy*, **185**; 165–188

Khan, I., D. Tan, W. Azam, and S. T. Hassan (2022). Alternate Energy Sources and Environmental Quality: The Impact of

Inflation Dynamics. *Gondwana Research*, **106**; 51–63
Kusumawati, N., P. Setiarso, A. B. Santoso, S. Muslim, Q. A'yun, and M. M. Putri (2023). Characterization of Poly (vinylidene Fluoride) Nanofiber-Based Electrolyte and Its Application to Dye-Sensitized Solar Cell with Natural Dyes. *Indonesian Journal of Chemistry*, **23**(1); 113
Kusumawati, N., P. Setiarso, M. M. Sianita, and S. Muslim (2018). Transport Properties, Mechanical Behavior, Thermal and Chemical Resistance of Asymmetric Flat Sheet Membrane Prepared from PSf/PVDF Blended Membrane on Gauze Supporting Layer. *Indonesian Journal of Chemistry*, **18**(2); 257–264
Lal, M., P. Sharma, and C. Ram (2021). Calcination Temperature Effect on Titanium Oxide (TiO_2) Nanoparticles Synthesis. *Optik*, **241**; 166934
Liu, F., F. Bin, J. Xue, L. Wang, Y. Yang, H. Huo, J. Zhou, and L. Li (2020). Polymer Electrolyte Membrane with High Ionic Conductivity and Enhanced Interfacial Stability for Lithium Metal Battery. *ACS Applied Materials & Interfaces*, **12**(20); 22710–22720
Liu, R., B. Yuan, S. Zhong, J. Liu, L. Dong, Y. Ji, Y. Dong, C. Yang, and W. He (2021). Poly (vinylidene Fluoride) Separators for Next-Generation Lithium Based Batteries. *Nano Select*, **2**(12); 2308–2345
Lobregas, M. O. S. and D. H. Camacho (2019). Gel Polymer Electrolyte System Based on Starch Grafted with Ionic Liquid: Synthesis, Characterization and Its Application in Dye-Sensitized Solar Cell. *Electrochimica Acta*, **298**; 219–228
Medvids, A., P. Onufrijevs, J. Kaupužs, R. Eglitis, J. Padgurskas, A. Zunda, H. Mimura, I. Skadins, and S. Varnagiris (2021). Anatase or Rutile TiO_2 Nanolayer Formation on Ti Substrates by Laser Radiation: Mechanical, Photocatalytic and Antibacterial Properties. *Optics & Laser Technology*, **138**(106898); 106898
Padmini, M., T. Balaganapathi, and P. Thilakan (2021). Mesoporous Rutile TiO_2: Synthesis, Characterization and Photocatalytic Performance Studies. *Materials Research Bulletin*, **144**(111480); 111480
Richhariya, G., B. C. Meikap, and A. Kumar (2022). Review on Fabrication Methodologies and Its Impacts on Performance of Dye-Sensitized Solar Cells. *Environmental Science and Pollution Research*, **29**(11); 15233–15251
Sabzi, M. and S. M. Anijdan (2019). Microstructural Analysis and Optical Properties Evaluation of Sol-Gel Heterostructured NiO-TiO_2 Film Used for Solar Panels. *Ceramics International*, **45**(3); 3250–3255
Saxena, P. and P. Shukla (2021). A Comprehensive Review on Fundamental Properties and Applications of Poly (vinylidene Fluoride)(PVDF). *Advanced Composites and Hybrid Materials*, **4**(1); 8–26
Semalti, P. and S. N. Sharma (2020). Dye Sensitized Solar Cells (DSSCs) Electrolytes and Natural Photo-Sensitizers: A Review. *Journal of nanoscience and nanotechnology*, **20**(6); 3647–3658
Setiarso, P., R. V. Harsono, and N. Kusumawati (2023). Fabrication of Dye Sensitized Solar Cell (DSSC) Using Combination of Dyes Extracted from Curcuma (*Curcuma xanthorrhiza*) Rhizome and Binahong (*Anredera cordifolia*) Leaf with Treatment in pH of the Extraction. *Indonesian Journal of Chemistry*, **23**(4); 924
Shirkavand, M., M. Bavir, A. Fattah, H. R. Alaei, and M. H. Tayarani Najaran (2019). Influence of TiO_2 Layer Thickness as Photoanode in Dye Sensitized Solar Cells. *AUT Journal of Electrical Engineering*, **51**(1); 101–110
Tontapha, S., P. Uppachai, and V. Amornkitbamrung (2021). Fabrication of Functional Materials for Dye-Sensitized Solar Cells. *Frontiers in Energy Research*, **9**; 641983
Venkatesan, S., Y. Chen, H. Teng, and Y. Lee (2022). Enhanced Adsorption on TiO_2 Photoelectrodes of Dye-Sensitized Solar Cells by Electrochemical Methods Dye. *Journal of Alloys and Compounds*, **903**(163959); 163959
Vural, G. (2020). Renewable and Non-Renewable Energy-Growth Nexus: A Panel Data Application for the Selected Sub-Saharan African Countries. *Resources Policy*, **65**(101568); 101568
Xie, Y., J. Wang, F. Ren, H. Shuai, and G. Du (2022). Nonmetallic Mineral as the Carrier of TiO_2 Photocatalyst: A Review. *Frontiers in Catalysis*, **2**; 806316
Yang, J., J. Liu, Y. Li, X. Yu, Z. Yi, Z. Zhang, F. Chi, and L. Liu (2022). A DSSC Electrolyte Preparation Method Considering Light Path and Light Absorption. *Micromachines*, **13**(11); 1930
Zhang, K., W. Zhao, Q. Liu, and M. Yu (2021). A New Magnetic Melt Spinning Device for Patterned Nanofiber. *Scientific Reports*, **11**(1); 8895
Zhou, R., S. Yang, E. Tao, L. Liu, and J. Qian (2022). The Defect is Perfect: MoS_2/TiO_2 Modified with Unsaturated Mo Vacancies to Construct Z-Scheme Heterojunction & Improve Mobility of e^-. *Journal of Cleaner Production*, **337**(130511); 130511

